Laser and Particle Beams (2002), *20*, 31–38. Printed in the USA.

DOI: 10.1017.S0263034602201044

Propagation issues and energetic particle production in laser–plasma interactions at intensities exceeding 10^{19} W/cm^2

M. BORGHESI,[1] D.H. CAMPBELL,[2] A. SCHIAVI,[2] O. WILLI,[2] M. GALIMBERTI,[3] L.A. GIZZI,[3] A.J. MACKINNON,[4] R.D. SNAVELY,[4] P. PATEL,[4] S. HATCHETT,[4] M. KEY,[4] AND W. NAZAROV[5]

[1]The Queen's University, Belfast BT7 1NN, UK
[2]Imperial College of Science, Technology and Medicine, London SW7 2BZ, UK
[3]Istituto di Fisica Atomica e Molecolare, CNR, 56100 Pisa, Italy
[4]Lawrence Livermore National Laboratory, Livermore, California 94550-9234, USA
[5]University of Dundee, Dundee DD1 4HN, UK

(RECEIVED 18 April 2001; ACCEPTED 2 October 2001)

Abstract

A series of experiments recently carried out at the Rutherford Appleton Laboratory investigated various aspects of the laser–plasma interaction in the relativistic intensity regime. The propagation of laser pulses through preformed plasmas was studied at intensities exceeding 10^{19} W/cm^2. The transmission of laser energy through long-scale underdense plasmas showed to be inefficient unless a plasma channel is preformed ahead of the main laser pulse. The study of the interaction with overdense plasmas yielded indication of collimated energy transport through the plasma. The production of fast particles during the interaction with solid density targets was also investigated. The measurements revealed the presence of a small-sized directional source of multi-megaelectron volt protons, which was not observed when a plasma was preformed at the back of the solid target. The properties of the source are promising in view of its use in radiographic imaging of dense matter, and preliminary tests were carried out.

Keywords: Laser-plasma interaction; Laser-produced ions; Proton; Radiography; Relativistic propagation

1. INTRODUCTION

The fast ignitor (FI) approach (Tabak *et al.*, 1994) to inertial confinement fusion motivates much of the present interest in ultraintense laser–plasma interaction studies. In fact, as the scheme relies on the energy of an extremely intense laser pulse to start ignition in a compressed capsule, the study of the propagation of ultraintense laser pulses through dense plasmas is of great relevance to the success of this scheme. Nonetheless, this type of study is of great topical interest also because of the novel and complex physics involved. In the ultrahigh-intensity regime, the laser undergoes highly nonlinear processes due to the relativistic behavior of the electrons oscillating in the laser field (Umstadter *et al.*, 1996). These phenomena can lead to a number of novel effects, including relativistic self-focusing (Esarey *et al.*, 1997 and references within), explosive channel formation (Borghesi *et al.*, 1998; Chen *et al.*, 1998; Fuchs *et al.*, 1998), and induced transparency of overdense plasmas (Lefebvre & Bonnaud, 1995; Cairns *et al.*, 2000). During interaction in the relativistic regime, a considerable fraction of the laser energy is deposited into highly energetic electrons (Malka *et al.*, 1997; Gahn *et al.*, 1999) and ions (Krushelnick *et al.*, 1999; Clark *et al.*, 2000). This paper reviews results obtained in an experimental campaign recently carried out at the VULCAN laser facility, Rutherford Appleton Laboratory (UK). In the chirped pulse amplification (CPA) mode, the VULCAN laser (Danson *et al.*, 1998) provides up to 75 J in 1-ps pulses at a wavelength of 1.054 μm. Various aspects of the interaction of relativistically intense pulses with preformed plasmas and solid targets were investigated in the experiments. In the following sections, the aims of the experiments, the techniques employed and the main results obtained will be described.

Address correspondence and reprint requests to: Dr. M. Borghesi, Department of Pure and Applied Physics, The Queen's University of Belfast, Belfast BT7 1NN, UK. E-mail: m.borghesi@qub.ac.uk

2. PROPAGATION THROUGH UNDERDENSE PLASMAS

A study of the propagation of ultraintense laser pulses through long-scale underdense plasmas was carried out. This is an extremely important issue for the fast ignitor scheme, as the transmission of laser energy through the coronal underdense plasma region surrounding the compressed target is a fundamental prerequisite for energy delivery to the core. The ignitor pulse has to propagate without loss of energy, and without being affected by filamentation. In fact, while in the subrelativistic regime absorption in underdense plasmas becomes less important as the intensity increases (Pert, 1995), the situation changes as the intensity enters the relativistic regime. Anomalously low energy transmission has been observed in experiments carried out with mid-10^{18} W/cm^2 pulses in moderately underdense plasmas (Cobble *et al.*, 1997). Recent theoretical work highlights the possibility for an underdense plasma slice to become opaque to ultraintense irradiation, and attributes the energy loss to the excitation of strong Raman-like parametric instabilities (Adam *et al.*, 2000). This reason makes the requirement of a trailing pulse to open a channel through the plasma ahead of the ignitor pulse extremely compelling even in the low density coronal region.

Extensive investigations of the propagation of relativistic pulses through underdense plasmas have been carried out by our group in previous experimental campaigns. Among the results obtained were direct observations of relativistic-ponderomotive self-channeling (Borghesi *et al.*, 1997) and Coulomb explosion, measurement of transient ultralarge magnetic fields due to the laser propagation (Borghesi *et al.*, 1998), and guiding of ultraintense pulses through channels formed by 10–20 ps pulses (Mackinnon *et al.*, 1999; Borghesi *et al.*, 2000).

The experimental arrangement for our measurements is shown in Figure 1. The plasmas were produced by exploding thin plastic foils (0.1, 0.3, or 0.5 μm thick) with 2-ns, 0.527-μm laser pulses at a total irradiance of about 5×10^{14} W/cm^2. After a suitable delay (typically of the order of 1 ns) the CPA pulse was focused into the plasma. At this time the peak density of the plasma was of the order of $n_c/10$ and its longitudinal extension was of the order of a millimeter (the peak densities have been estimated using a self-similar model for the plasma expansion (London & Rosen, 1986)). With $f/3.5$ focusing optics, the CPA vacuum irradiance was up to 5×10^{19} W/cm^2 (about 50 J on target, with up to 50% of the energy in a 10–15-μm focal spot). A fraction of the energy of the main CPA pulse was used to provide a prepulse, collinear with the main pulse. The prepulse could be focused into the plasma ahead of the main pulse and used to open a density channel. A further small fraction of the CPA pulse was frequency quadrupled and used as a transverse optical probe.

A set of photomultiplier coupled with scintillating crystals (thickness ranging from 12.5 to 50 mm) was placed outside the interaction chamber along the direction of the transmitted CPA pulse to detect forward-emitted γ-rays. This is mainly brehmsstrahlung radiation emitted by energetic electrons slowed down by objects placed on their path, for example, calorimeter, interaction chamber walls, and so forth. Other diagnostics included calorimetry of the energy transmitted through the plasma, imaging of the transmitted laser spot, and forward and back-scatter spectroscopy.

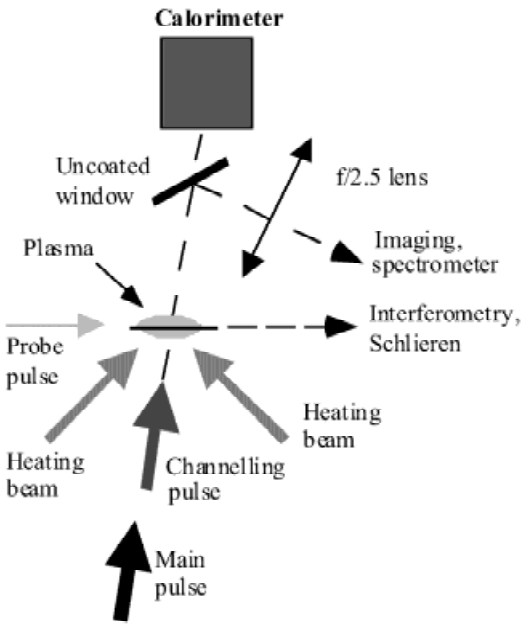

Fig. 1. Experimental arrangement for studies of ultraintense propagation through underdense plasmas.

The propagation of the main CPA pulse through the plasma was first studied without a preformed plasma channel. The energy transmission through the plasma in this case was very low. Even when using 0.1-μm targets, which gave a plasma with a peak density of a few times $n_c/100$, the energy transmitted was limited to a few percent of the laser energy incident on target. The low energy transmission may also be related to the onset of relativistic filamentation (Young & Bolton, 1996; Wang *et al.*, 2000) rather than whole-beam self-focusing. Relativistic filamentation can cause spreading of the beam energy at angles much larger than the focusing angle and has been correlated with more efficient energy transfer into hot electrons. Filamentation and beam spreading was indeed observed in the experiment, as clear, for example, in Figure 2, showing an interferogram taken 5 ps after the interaction of a 50-TW pulse with the plasma.

The effect of the presence of a preformed channel on the propagation of the main pulse was investigated. The channel was formed by focusing into the plasma a prepulse with a prepulse-to-main ratio of 1:2. The intensity of the prepulse was also above 10^{19} W/cm^2, and a rapidly expanding channel was formed via ponderomotive expulsion of the electrons and subsequent Coulomb explosion, as observed in previous experiments (Borghesi *et al.*, 1997, 1998; Fuchs *et al.*, 1998). The CPA main pulse transmittance was mea-

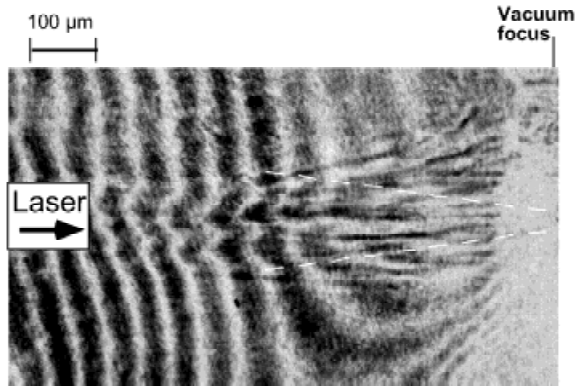

Fig. 2. Interferogram taken 5 ps after the propagation of a 50-TW pulse through the plasma (peak density ~0.1 n_c). Many filaments are visible on the right side of the figure. The dashed white line indicates the cone defined by the focusing optics.

sured, for various plasma conditions, as a function of the delay between the main and the channeling pulse (see Fig. 3). The energy transmitted through the plasma grows from the few percent transmittance measured in the absence of a preformed channel to almost 100% transmission when the channeling-to-main delay is of the order of 100 ps. The enhanced transmission can be ascribed to the combination of various factors. The density inside the channel is considerably lower than the plasma background density, and this determines a decrease of the energy depletion (anomalous absorption) and scattering (filamentation, transverse wakefield) mechanisms. While in the first tens of picoseconds after the interaction the density profile inside the channel looks somehow perturbed, at later times, the interaction pulse will propagate in a smooth profile with a minimum on

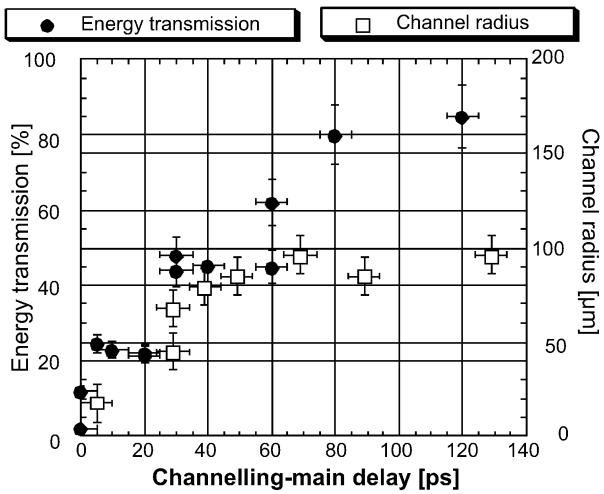

Fig. 3. Energy transmission through an underdense plasma (peak density ≈ 0.03 n_c, length ≈ 1–2 mm, obtained from explosion of 0.1-μm targets) in the presence of a preformed channel. The transmission is plotted versus the delay between the channel formation and the propagation of the main pulse. The temporal evolution of the channel radius is also plotted.

axis. Therefore the density profile will act as a a waveguide on the pulse. When interpreting the data, it is important to remember that the energy distribution in the focal plane of the laser will be such that, typically, only 30–40% of the energy is contained in the small size high-intensity central spot (10–20 μm diameter). The rest of the energy is distributed throughout lower intensity wings extending around the spot. Therefore the 20% transmission achieved even after 10–20 ps means that more than half of the energy contained in the high intensity portion of the focal spot has been transmitted. As the channeling-to-main delay is increased, the transmission further increases: As a matter of fact, as the channel diameter increases (see Fig. 3), the lower intensity, larger diameter wings of the focal spot start to be contained within the channel walls. The internal dynamics of the channel (e.g., the temporal evolution of the density inside the channel) will also play a role. Detailed modeling is required to determine the relative importance of the different factors.

A similar trend for the transmission has been observed through denser plasmas, obtained by exploding 0.3-μm targets. The overall transmission is lower, due to less efficient channel formation over the whole plasma length, as a consequence of the higher density of the plasma.

γ-ray measurements (Galimberti *et al.*, 2001; Gizzi *et al.*, 2001) seem to confirm the transition from a regime of strong filamentation when no guiding is provided to a regime of efficient interaction over an extended distance in presence of a preformed channel. The data, obtained with plasmas with peak density of the order of 01–0.2 n_c, are shown in Figure 4.

When no guiding is provided, a large signal with a very high shot-to-shot variability was observed. This is consistent with a disordered and chaotic interaction as would take place in a strong filamentation regime. The laser light in the filaments can reach high intensities and generate efficiently jets of hot electrons, with random orientation.

When the interaction pulse propagated in the preformed channel, much more reproducible data was obtained. The signal, which for 20-ps delay was generally lower than in the single-pulse case, increased when the delay between channel formation and propagation was increased (in the range 20–120 ps). Analysis of the channel density profile (Gizzi *et al.*, 2001) confirmed that the efficiency of the acceleration process is related to the smoothing of the density profile inside the channel. Density perturbations present at early times disappear at a later stage of the channel evolution and the pulse propagates in an uniform low-density plasma with gently rising edges.

3. INTERACTION WITH PREFORMED OVERDENSE PLASMAS

The interaction of the Vulcan CPA pulse with slightly overdense preformed plasmas was also investigated. This is a regime of interaction of particular interest for comparison with computational models, which has not received much experimental attention yet, mainly due to the difficulty of

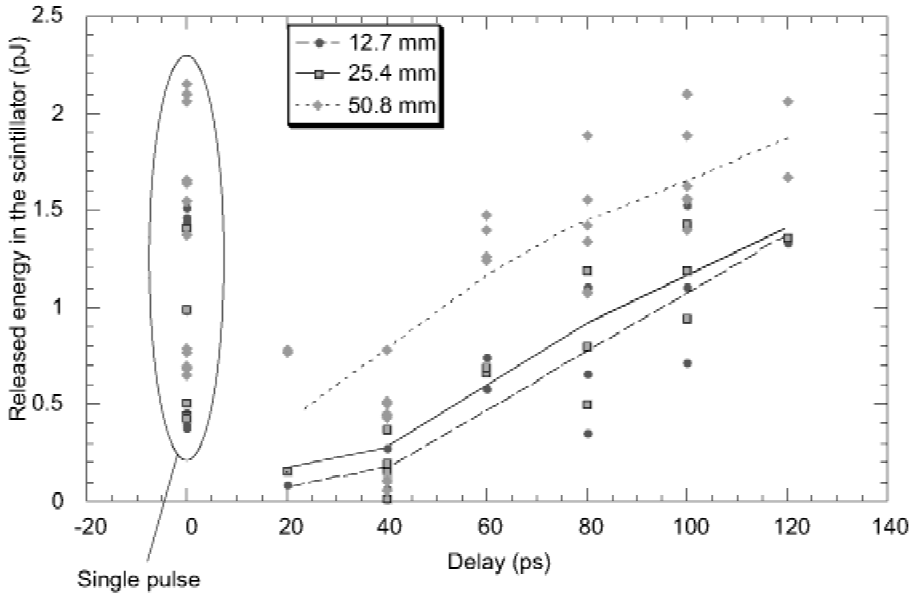

Fig. 4. Energy released by the gamma-ray photons in the detector scintillating crystal as a function of the delay between the channel-forming pulse and the main CPA pulse for three different values of the thickness of the crystal. The data refer to interaction with plasmas formed by exploding 0.1 and 0.3 μm targets (i.e., peak densities in the range 0.03–0.1 n_c). The signal for zero delay corresponds to interactions in which no channel was preformed ahead of the interaction pulse.

providing controllable plasmas with the required characteristics. The physics of the interaction in this regime is, for obvious reasons, very different than in the underdense plasmas. Although classically normally incident laser light should be reflected at the critical surface (i.e., when the density is such that the laser frequency equates the plasma frequency), relativistic effects may allow propagation of the laser pulse up to densities higher than critical (Kaw & Dawson, 1970; Lefebvre & Bonnaud, 1995; Cairns *et al.*, 2000). Ponderomotive effects will also be effective in setting the critical surface in forward motion in the focal spot region, favoring the laser pulse propagation (Wilks & Kruer, 1997). In a realistic interaction condition, however, depletion of the pulse energy (Pukhov *et al.*, 1997) will seriously limit the propagation, even at plasma densities that are below the relativistically enhanced critical density. The study of the propagation of laser-produced energetic electrons in the dense plasmas is also of great interest, particularly in the fast ignitor context. Similar studies have been carried out up to now with solid targets, providing evidence of collimation of megaelectron volt fast electrons accelerated in the interaction region (Tatarakis, 1998; Borghesi *et al.*, 1999; Gremillet *et al.*, 1999).

In our experiment, the overdense plasmas were preformed via X-ray heating of low density CH foams, with densities in the range 10–30 mg/cc. The X-rays were produced by irradiating two 700Å Au foils with 600-ps, 0.527-μm pulses focused at an irradiance of 5×10^{14} W/cm^2. The use of foam targets provided a relatively uniform plasma with controllable density and temperature, without the strong density gradients affecting dense plasmas obtainable from solid targets. The CPA pulse was focused into the plasma with variable delay after the plasma formation, typically 0.6 to 1 ns after the plasma formation. The density of the foam targets insured that the plasma was overdense for the CPA pulse (between 2 and 6 n_c depending on the target used). The length of the foams varied between 100 and 200 μm.

The X-ray emission from the plasma in the kiloelectron volt range was imaged with two pinhole cameras, with magnification, respectively, of 10 and 20. The back of the foam was imaged with a $f/2.5$ lens, and shadowgrams of the target were obtained using the transverse UV picosecond probe. Filamentary X-ray emission was observed to extend throughout the foam along the laser propagation axis. X-ray images from the rear and front pinhole cameras show bright filaments extending through the foam and some distance beyond. Such filaments are observed on several shots for different foam densities and lengths. Transverse optical probing revealed localized explosion of the back surface of the target, in line with the CPA propagation axis.

Modeling currently in progress attributes the X-ray emission to localized heating of the plasma due to a hot electron jet drawing a return current from the plasma, in an analogous way to what is observed in solid transparent targets (Borghesi *et al.*, 1999).

4. PRODUCTION OF MULTI-MEGAELECTRON VOLT PROTONS

One of the most exciting results recently obtained in this area of research is the observation of very energetic beams of protons, generated during the interaction of ultraintense

short pulses with solid targets. In a number of experiments, performed with different laser systems and in different interaction conditions, protons with energies up to several tens of megaelectron volts have been detected behind thin foils irradiated with high-intensity pulses (Clark *et al.*, 2000; Maksimchuk *et al.*, 2000; Snavely *et al.*, 2000). In these experiments, it was seen that the particle beams are directed along the normal to the back surface of the target, and have a small angular aperture at the highest energies. As proton beams are observed even using targets which nominally do not contain hydrogen, protons are thought to originate from hydrocarbon impurities located on the target surfaces or from bulk contamination of the target. There has been a strong debate whether the source of the energetic protons is located at the front or at the back surface of the solid target. Arguments based on the angular distributions of the proton energy across the beam have been used by Clark *et al.* (2000) to support the hypothesis of a proton source located at the front surface of the target. On the other hand, the fact that the proton beam is perpendicular to the target back surface (rather than collinear with the interaction beam) supports the hypothesis that the proton acceleration takes place at the back of the target (Snavely *et al.*, 2000). In this case, the protons would be accelerated by the enormous electric field (approximately megavolts/micron) set up by the fast electrons leaving the target (Hatchett *et al.*, 2000; Wilks *et al.*, 2001).

The particular properties of these beams (small source size, high degree of collimation, short duration, energy dependence on the target characteristics) make them of particular interest in view of possible applications. Among these, their use as the ignition trigger in the fast ignitor scheme (Roth *et al.*, 2001) and as a probe in high-density matter investigations (Borghesi *et al.*, 2001) have been proposed.

The protons were produced by focusing the CPA pulse onto 25-μm-thick Al foils, and detected using layers of radiochromic film (RCF; McLaughlin *et al.*, 1991) and plastic tracks detectors (Enge, 1995) placed in a stack at the back of the target, typically at a distance of about 2 cm. It was found that the proton beams have high brightness, typically with 10^{12} protons with energy above 3 MeV per shot (for laser irradiance of the order of 5×10^{19} Wcm^{-2}). As observed in previous experiments, the beams were highly directional, propagating along the normal to the back surface of the target with small angular divergence (about 15° for 10 MeV protons). RC film data for a typical proton beam generated from a 25-μm Al foil is shown in Figure 5(a). The proton beam is the distinct feature at the top edge of the film, while the diffuse background is due to energetic electrons. The fact that only half of the proton beam is visible on the

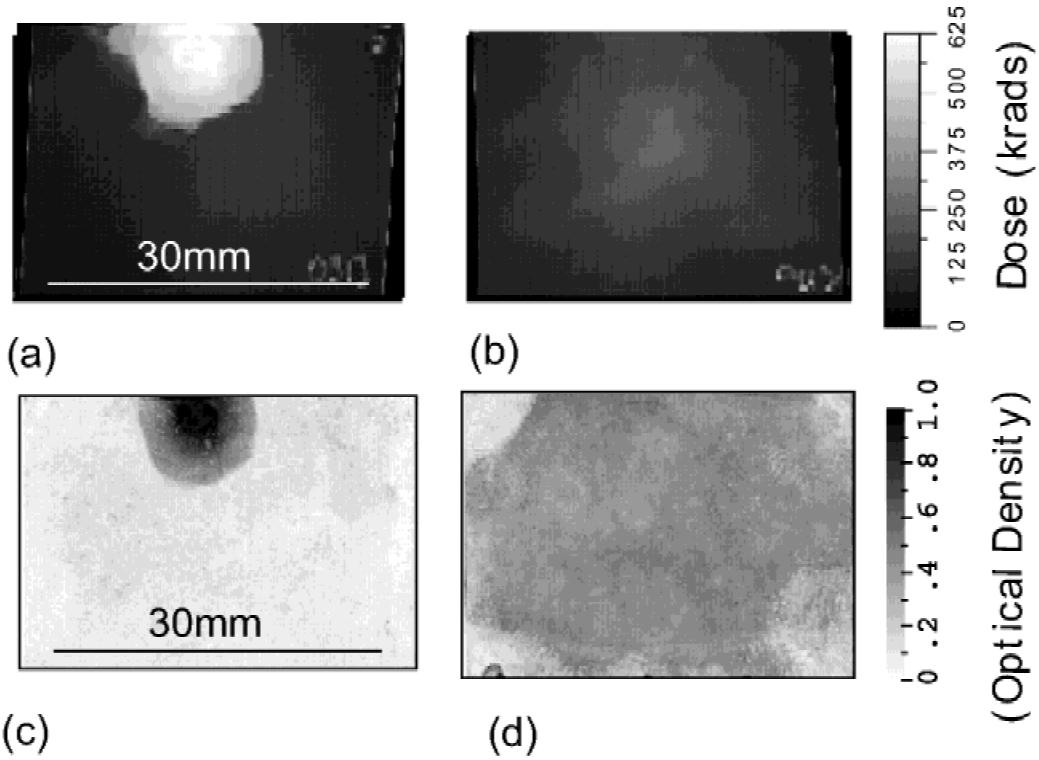

Fig. 5. Radiochromic film data for proton energies between 9.5 and 10 MeV in the case of (a) an unperturbed target and (b) a target with a 100-μm ion density scale length plasma at the back surface. Etched Mylar layer corresponding to the case of (c) no preformed plasma and (d) preformed plasma at the back of the target.

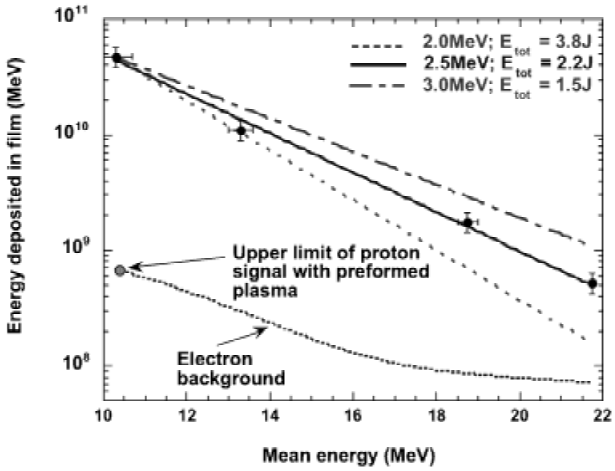

Fig. 6. Proton energy deposited in the various RCF layers (data of Fig. 5a) plotted versus the mean energy of the protons reaching the Bragg peak in the layer; the curve at the bottom of the plot indicates the amount of energy deposited by the background electrons in the RCF layers in the case of Fig. 5b. As no protons signal is visible above the noise, the electron dose can be used to overestimate the dose deposited by the protons.

film is due to setup constraints in placing the RC film in this particular shot. The response of each layer to high-energy protons has been determined using Monte Carlo modeling of the deposited energy by the particles. Each film layer, except the first, responds to ions within an energy band of less than 1 MeV. The layer shown in Figure 5(a) represents proton energies between 9.5 and 10 MeV. A strong proton signal was observed out to the layer corresponding to proton energy just above 20 MeV. This cutoff is in quantitative agreement with the data presented by Clark *et al.* (2000), which were obtained using the same Vulcan laser facility. The energy deposited within each film layer can be extracted from the absolutely calibrated film. By doing this for each film layer and fitting an exponential energy dependence, an estimate of the proton energy spectrum and total energy can be extracted from the film data. Figure 6 shows the energy deposited (in megaelectron volts) in the film as a function of proton energy. The plot is for all RCF layers apart from the first. The best fit to the data in these RCF layers is also shown. The mean proton energy of the exponential fit is 3.75 MeV $\pm$ 0.3 MeV with a total energy of 2.2 J in an equivalent Maxwellian with a temperature of 2.5 MeV.

During the experiments, the source size of the proton beam was estimated using a penumbral edge method, setting an upper limit of 15–20 μm diameter for the source of 10 MeV protons. It is presently unclear whether the observed source is real or rather a virtual one (with the protons emitted from a larger area with finite angular divergence and spread). In any case, the measured source size is small enough to permit the implementation of point projection imaging schemes, and sets the spatial resolution of imaging applications.

A test was carried out to investigate the proton acceleration mechanism, and in particular its dependence on the scale length of the plasma at the back of the target (Mackinnon *et al.*, 2001). This was done to confirm the assumption that the protons are electrostatically accelerated at the back surface of the target. To create a finite plasma scale length, a preformed plasma was created by focusing a 600-ps-duration laser pulse at $\lambda = 0.527$ μm onto the back surface of the foil with an $f/10$ lens. The heating pulse energy, focal spot, and relative timing were all controlled on a shot-to-shot basis. For most shots, the energy on target was 10-J within a focal spot of 300 μm (FWHM), and the heating pulse started 250 ps before the interaction pulse, thus giving a mean intensity on target of 3×10^{13} Wcm^{-2}. As a matter of fact, the proton production was very different when the heating pulse was incident on the back surface of the foil, 250 ps prior to the arrival of the interaction pulse, and formed a plasma with a scale length at critical of the order of 20–50 μm. The RC data for this case is shown in Figure 5G. It can be seen that there is no evidence of a proton beam after the first RC film layer. This would set an upper limit of 10 MeV for the energy cut-off of the proton beam. Confirmation that the proton signal was very much reduced in the preformed plasma case was obtained by etching one of the three Mylar layers between the first two RC film layers. There was a one to one correspondence between the track features in the etched Mylar and the RC data. For the unperturbed case, in each layer the track density within the proton beam was very high and the signal fell off very sharply at the edge region of the spot. In contrast, for the preformed plasma case, the track density is high only on the first Mylar layer and it drops off very rapidly to background levels before the second layer of RC film. From this we can infer that the energy cut-off is actually lower than 5–6 MeV. The same behavior was observed in recent measurements when much thicker targets (up to 250 μm thick) were used. Even in this case the proton beam disappeared completely when a small plasma (with scale length of a few tens of microns) was produced on the back of the target, as predicted by electrostatic acceleration in the Debye sheath at the back surface of the target (Hatchett et al., 2000; Wilks *et al.*, 2001).

The beam was then used to carry out preliminary work on proton probing of solids and dense plasmas (Borghesi *et al.*, 2001).

The proton beam was applied to probing large-scale laser-produced plasmas, both in face-on and side-on configurations. Very interesting effects were observed: The intensity profile was modulated and presented repeatable patterns, which changed when the parameters of the plasma-producing laser pulse were changed. The structures are likely to be due to microfields related to density dishomogeneities imprinted by the heating pulse. The control of these nonuniformities is of great importance for inertial confinement fusion studies, where the uniformity of target compression is a fundamental requirement. This is an important investigation, also, in view of the possible use of proton beams to start ignition in alter-

native fast ignitor schemes for inertial confinement fusion recently proposed.

Finally, the short duration of the proton pulse was exploited to detect transient charge-up of solid targets following ultraintense interaction. The tests showed that the *proton imaging* technique has great potential as a plasma diagnostic, enabling, for example, direct measurements of electric fields in dense plasmas.

5. CONCLUSIONS

A series of issues related to the interaction physics in the relativistic intensity regime has been investigated in experiments recently carried out at the Rutherford Appleton Laboratory, employing the VULCAN laser in the operation mode. These studies are of great relevance to the fast ignitor concept, and indicate other possible applications. The results provided evidence of opacity of underdense plasmas to ultraintense radiation. It was also seen that the energy transmission and the quality of the interaction could be significantly increased by preforming a channel with a trailing pulse ahead of the main interaction pulse. Evidence of collimated energy transport in overdense plasmas was obtained in experiments using X-ray-heated foam targets. Finally, the generation of proton beams emitted from ultraintense interaction with thin solid targets was studied, revealing that the main acceleration mechanism takes place at the back surface of the target. The multi-megaelectron volt laser-produced proton beam was used as a particle probe or the first time to investigate field structures in plasmas and laser-irradiated solids.

ACKNOWLEDGMENTS

We thank the staff of the Rutherford Appleton Laboratory for the invaluable help provided in preparing and carrying out the experiment. This work was funded by an ESPRC grant.

REFERENCES

Adam, J.C., Heron, A., Laval, G. & Mora, P. (2000). Opacity of an underdense plasma slab due to the parametric instabilities of an ultraintense laser pulse. *Phys. Rev. Lett.* **84**, 3598–3601.

Borghesi, M., Campbell, D.H., Gessner, H., Schiavi, A., Willi, O., Mackinnon, A.J., Patel, P., Snavely, R., Hatchett, S., Gizzi, L.A., Galimberti, M., Clarke, R.J., Allott, R., Hawkes, S. & Ruhl, H. (2001). Fast particle generation in ultra-intense interaction experiments and applications. *Proceedings of the International Conference on Lasers 2000* (Corcoran, V.J. & Corcoran, T.S., Eds.), pp. 451–459. McLean, VA: STS Press.

Borghesi, M., Mackinnon, A.J., Barringer, L., Gaillard, R., Gizzi, L.A., Meyer, C., Willi, O., Pukhov, A. & Meyer-ter-Vehn, J. (1997). Relativistic channelling of a picosecond laser pulse in a near-critical preformed plasma. *Phys. Rev. Lett.* **78**, 879–883.

Borghesi, M., Mackinnon, A.J., Bell, A.R., Malka, G., Vickers, C., Willi, O., Davies, J.R., Pukhov, A. & Meyer-ter-Vehn, J. (1999). Observations of collimated ionization channels in solid glass irradiated by ultrahigh intensity laser pulses. *Phys. Rev. Lett.* **83**, 4309–4312.

Borghesi, M., Mackinnon, A.J., Gaillard, R., Willi, O., Pukhov, A. & Meyer-ter-Vehn, J. (1998). Large, quasistatic magnetic fields generated by a relativistically intense laser pulse propagating in a preformed plasma. *Phys. Rev. Lett.* **80**, 5137–5141.

Borghesi, M., Mackinnon, A.J., Gaillard, R., Malka, G., Vickers, C., Willi, O., Miquel, J.L., Blanchot, N., Canaud, B., Davies, J.R., Pukhov, A. & Meyer-ter-Vehn, J. (2000). Short pulse interaction experiments for fast ignitor applications. *Laser Part. Beams* **18**, 389–397.

Cairns, R.A., Rau, B. & Airila, M. (2000). Enhanced transmission of laser light through thin slabs of overdense plasmas. *Phys. Plasmas* **7**, 3736.

Chen, S.Y., Sarkisov, G.S., Maksimchuk, A., Wagner, R. & Umstadter, D. (1998). Evolution of a plasma waveguide created during relativistic-ponderomotive self-channeling of an intense laser pulse. *Phys. Rev. Lett.* **80**, 2610.

Clark, E.L, Krushelnick, K., Davies, J.R., Zepf, M., Tatarakis, M., Beg, F.N., Machacek, A., Norreys, P.A., Santala, M.I.K., Watts, I. & Dangor, A.E. (2000). Measurements of energetic proton transport through magnetized plasma from intense laser interactions with solids. *Phys. Rev. Lett.* **84**, 670–673.

Cobble, J.A., Johnson, R.P. & Mason, R.J. (1997). High-intensity illumination of an exploding foil. *Phys. Plasmas* **4**, 3006–3011.

Danson, C.N. Collier, J., Neely, D., Barzanti, L.J., Damerell, A., Edwards, C.B., Hutchinson, M.H.R., Key, M.H., Norreys, P.A., Pepler, D.A., Ross, I.N., Taday, P.F., Toner, W.T., Trentelman, M., Walsh, F.N., Winstone, T.B. & Wyatt, R.W.W. (1998). Well characterized 10^{19} W cm^2 operation of VULCAN—An ultra-high power Nd:glass laser. *J. Mod. Opt.* **45**, 1653–1669.

Enge, W. (1995). On the question of nuclear track formation in plastic material. *Rad. Meas.* **25**, 11–25.

Esarey, E., Sprangle, P., Krall, J. & Ting, A. (1997). Self-focusing and guiding of short laser pulses in ionizing gases and plasmas. *IEEE J. Quantum Electron.* **33**, 1879–1914.

Fuchs, J., Malka, G., Adam, J.C., Amiranoff, F., Baton, S.D., Blanchot, N., Heron, A., Laval, G., Miquel, J.L., Mora, P., Pepin, H. & Rousseaux, C. (1998). Dynamics of subpicosecond relativistic laser pulse self-channeling in an underdense preformed plasma. *Phys. Rev. Lett.* **80**, 1658–1661.

Gahn, C., Tsakiris, G.D., Pukhov, A., Meyer-ter-Vehn, J., Pretzler, G., Thirolf, P., Habs, D. & Witte K.J. (1999). Multi-MeV electron beam generation by direct laser acceleration in high-density plasma channels. *Phys. Rev. Lett.* **83**, 4772–4775.

Galimberti, M., Giulietti, A., Giulietti, D., Gizzi, L.A., Borghesi, M., Campbell, D.H., Schiavi, A. & Willi, O. (2001). Gamma-ray measurements in relativistic interactions with underdense plasmas. *Proc. SPIE* **4424**, 512–515.

Gizzi, L.A., Galimberti, M., Giulietti, A., Giulietti, D., Tomassini, P., Borghesi, M., Campbell, D.H., Schiavi, A. & Willi, O. (2001). Relativistic laser interactions with preformed plasma channels and gamma-ray measurements. *Laser Part. Beams* **19**, 181–186.

Gremillet, L., Amiranoff, F., Baton, S.D., Gauthier, J.-C., Koenig, M., Martinolli, E., Pisani, F., Bonnaud, G., Lebourg, C., Rousseaux, C., Toupin, C., Antonicci, A., Batani, D., Bernardinello, A., Hall, T., Scott, D., Norreys, P., Bandulet, H. & Pépin, H. (1999). Time-resolved observation of ultrahigh intensity laser-produced electron jets propagating through transparent solid targets. *Phys. Rev. Lett.* **83**, 5015.

Hatchett, S.P., Brown, C.G., Cowan, T.E., Henry, E.A., Johnson, J.S., Key, M.H., Koch, J.A., Langdon, A.B., Lasinski, B.F., Lee, R.W., Mackinnon, A.J., Pennington, D.M., Perry, M.D., Phillips, T.W., Roth, M., Sangster, T.C., Singh, M.S. & Yasuike, R. (2000). Electron, photon, and ion beams from the relativistic interaction of petawatt laser pulses with solid targets. *Phys. Plasmas* **7**, 2076–2082.

Kaw, P. & Dawson, P. (1970). Relativistic nonlinear propagation of laser beams in cold overdense plasmas. *Phys. Fluids* **13**, 472–481.

Krushelnick, K., Clark, E.L., Najmudin, Z., Salvati, M., Santala, M.I.K., Tatarakis, M., Dangor, A.E., Malka, V., Neely, D., Allott, R. & Danson, C. (1999). Multi-MeV ion production from high-intensity laser interactions with underdense plasmas. *Phys. Rev. Lett.* **83**, 737–740.

Lefebvre, E. & Bonnaud, G. (1995). Transparency/opacity of a solid target illuminated by an ultrahigh-intensity laser pulse. *Phys. Rev. Lett.* **74**, 2002–2005.

London, R.A. & Rosen, M.D. (1986). Hydrodynamics of exploding foil X-ray lasers. *Phys. Fluids* **29**, 3813–3822.

Mackinnon, A.J., Borghesi, M., Hatchett, S., Key, M.H., Patel, P., Campbell, D.H., Schiavi, A., Snavely, R. & Willi, O. (2001). Effect of plasma scalelength on multi-MeV proton production by intense laser pulses. *Phys. Rev. Lett.* **86**, 1769–1772.

Mackinnon, A.J., Borghesi, M., Gaillard, R., Malka, G., Willi, O., Pukhov, A., Meyer-ter-Vehn, J., Miquel, J.L., Blanchot, N. & Canaud, B. (1999). Intense laser pulse propagation and channel formation through plasmas relevant for the fast ignitor scheme. *Phys. of Plasmas* **6**, 2185–2190.

Maksimchuk, A., Gu, S., Flippo, K., Umstadter, D. & Bychenkov, V.Yu. (2000). Forward ion acceleration in thin films driven by a high-intensity laser. *Phys. Rev. Lett.* **84**, 4108–4111.

Malka, G., Fuchs, J., Amiranoff, F., Baton, S.D., Gaillard, R., Miquel, J.L., Pepin, H., Rousseaux, C., Bonnaud, G., Busquet, M. & Lours, L. (1997). Effect of plasma scalelength on multi-MeV proton production by intense laser pulses. *Phys. Rev. Lett.* **79**, 2053–2056.

McLaughlin, W.L., Humphreys, J.C., Hocken, D. & Chappas, W.J. (1991). Sensitometry of the response of a new radiochromic film dosimeter to gamma-radiation and electron-beams. *Nucl. Instrum. Methods. Phys. Res. A* **302**, 165–176.

Pert, G.J. (1995). Inverse bremsstrahlung in strong radiation-fields at low-temperatures. *Phys. Rev. E* **51**, 4778–4789.

Pukhov, A. & Meyer-terehn, J. (1997). Laser hole boring into overdense plasma and relativistic electron currents for fast ignition of ICF targets. *Phys. Rev. Lett.* **79**, 2686–2689.

Roth, M., Cowan, T.E., Key, M.H., Hatchett, S.P., Brown, C., Fountain, W., Johnson, J., Pennington, D.M., Snavely, R., Wilks, S.C., Yasuike, K., Ruhl, H., Pegoraro, F., Bulanov, S.V., Campbell, E.M., Perry, M.D. & Powell, H. (2001). Fast ignition by intense laser-accelerated proton beams. *Phys. Rev. Lett.* **86**, 436–439.

Snavely, R.A., Key, M.H., Hatchett, S.P., Cowan, T.E., Roth, M., Phillips, T.W., Stoyer, M.A, Henry, E.A., Sangster, T.C., Singh, M.S., Wilks, S.C., Mackinnon, A., Offenberger, A., Pennington, D.M., Yasuike, K., Langdon, A.B., Lasinski, B.F., Johnson, J., Perry, M.D. & Campbell, E.M. (2000). Intense high-energy proton beams from petawatt-laser irradiation of solids. *Phys. Rev. Lett.* **85**, 2945–2948.

Tabak, M., Hammer, J., Glinsky, M.E., Kruer, W.L., Wilks, S.C., Woodworth, J., Campbell, E.M., Perry, M.D. & Mason, R.J. (1994). Ignition and high gain with ultrapowerful lasers. *Phys. Plasmas* **1**, 1626–1634.

Tatarakis, M., Davies, J.R., Lee, P., Norreys, P.A., Kassapakis, N.G., Beg, F.N., Bell, A.R., Haines, M.G. & Dangor, A.E. (1998). Plasma formation on the front and rear of plastic targets due to high-intensity laser-generated fast electrons. *Phys. Rev. Lett.* **81**, 999–1002.

Umstadter, D., Chen, S.Y., Maksimchuk, A., Mourou, G. & Wagner, R. (1996). Nonlinear optics in relativistic plasmas and laser wake field acceleration of electrons. *Science* **273**, 472–475.

Wang, X. Krishnan, M., Saleh, N., Wang, H. & Umstadter, D. (2000). Electron acceleration and the propagation of ultrashort high-intensity laser pulses in plasmas. *Phys. Rev. Lett.* **84**, 5324–5327.

Wilks, S.C. & Kruer, W.L. (1997). Absorption of ultrashort, ultra-intense laser light by solids and overdense plasmas. *IEEE J. Quant. Electron.* **33**, 1954–1968.

Wilks, S.C, Langdon, A.B., Cowan, T.E., Roth, M., Singh, M., Hatchett, S., Key, M.H., Pennington, D., Mackinnon, A. & Snavely, R.A. (2001). Energetic proton generation in ultra-intense laser-solid interactions. *Phys. Plasmas* **8**, 542–549.

Young, P.E. & Bolton, P.R. (1996). Propagation of subpicosecond laser pulses through a fully ionized plasma. *Phys. Rev. Lett.* **77**, 4556–4559.